

Construction of $bb\bar{u}\bar{d}$ tetraquark states on lattice with NRQCD bottom and HISQ up/down quarks

Protick Mohanta and Subhasish Basak

School of Physical Sciences, National Institute of Science

Education and Research, HBNI, Odisha 752050, India

(Dated: August 26, 2020)

Abstract

We construct $bb\bar{u}\bar{d}$ states on lattice using NRQCD action for bottom and HISQ action for the light up/down quarks. The NRQCD-HISQ tetraquark operators are constructed for “bound” $[bb][\bar{u}\bar{d}]$ and “molecular” $[b\bar{u}][b\bar{d}]$ states. Corresponding to these different operators, two different appropriately tuned light quark masses are needed to obtain the desired spectra. We explain this requirement of different $m_{u/d}$ in the light of relativised quark model involving Hartree-Fock calculation. The mass spectra of double bottom tetraquark states are obtained on MILC $N_f = 2 + 1$ Asqtad lattices at three different lattice spacings. Variational analysis has been carried out to obtain the relative contribution of “bound” and “molecular” states to the energy eigenstates.

I. INTRODUCTION

The multiquark hadronic states other than the mesons and baryons are relatively new entrants particularly in the heavy quark sector. The signature of some of such states containing four or more quarks and/or antiquarks have been observed in experiments [1–6]. Such states are characterized by J^{PC} quantum numbers that cannot be arrived at from the quark model. (Such four quark states are popularly referred to as tetraquark, which is used to denote either bound or often both bound and mesonic molecular states. In this paper we use the term tetraquark in the latter sense.) However, heavy hadronic tetraquark states $Q\bar{Q}l\bar{l}$ and their stability in the infinite quark mass limit had been studied in [7, 8] which raised the possibility of existence of heavy four quark bound states below the $Q\bar{l} - Q\bar{l}$ threshold. Of late, the observations of $Z^-(4430, 1^+)$ of minimal quark content being $c\bar{c}d\bar{u}$ [3] have been reported along with the 1^+ states like $Z_b(10610)$ and $Z'_b(10650)$, having minimal quark content of four quarks (containing a $b\bar{b}$ pair) that are a few MeV above the thresholds of $B^*\bar{B}$ (10604.6) and $B^*\bar{B}^*$ (10650.2) [1, 2]. The proximity of Z_b , Z'_b to the $B^*\bar{B}^*$ threshold values perhaps suggest molecular, instead of bound, nature of the states.

Around the same time, lattice QCD has been employed to investigate the bound and/or molecular nature of the heavy tetraquark states, not only to understand the above experimentally observed states but also to identify other possible bound tetraquark states in both 0^+ and 1^+ channels. In the charm sector, some early lattice studies involve T_{cc} and T_{cs} tetraquark states [9], $ccc\bar{c}$ [10], $X(3872)$ and $Y(4140)$ [11] and more recently $D_{s0}^*(2317)$ [12]. The bottom sector received intense attention where, instead of $B^*\bar{B}$ or $B^*\bar{B}^*$, relatively simpler BB , BB^* systems are studied. The lattice investigations this far involve four bottom $bb\bar{b}\bar{b}$ [13] and two bottom tetraquark states $\bar{b}\bar{b}l_1l_2$, where $l_1, l_2 \in c, s, u, d$, [14–17]. An important observation of these lattice studies is that the possibility of the existence of $bb\bar{l}_1\bar{l}_2$ tetraquark bound states increases with decreasing light quark masses, while they become less bound with decreasing heavy (anti)quark mass.

Besides the usual lattice simulations, the heavy tetraquark systems have also been studied using QCD potential and Born-Oppenheimer approximation [18–21]. The main idea in this method is to investigate tetraquark states with two heavy (anti)quarks, which was $\bar{b}\bar{b}$ in the study, and two lighter quarks using quantum mechanical Hamiltonian containing screened Coulomb potential. This approach has been used to explain our two different choices of light

u/d quark masses for different classes of tetraquark states.

In this work our goal is to construct tetraquark states, having quark content $bb\bar{l}_1\bar{l}_2$ in 1^+ both below and above $B - B^*$ threshold, by a combination of lattice operators and tuning quark masses based on quantum mechanical potential calculation. For the b quark, we employed nonrelativistic QCD formulation [22, 23], as is the usual practice, and HISQ action [24] for $l_1, l_2 = u/d$. Here we also explore through variational/GEVP analysis how the trial states created by our operators contribute to the energy eigenstates.

First, we briefly review the salient features and parameters of both NRQCD and HISQ actions along with the steps involve in combining the relativistic u/d HISQ propagators with the NRQCD b quark propagators in the section II. We have considered two different kind of operators – the local heavy diquark and light antidiquark (often referred as “good diquark” configuration) and molecular meson-meson, we described these constructions in the section III. We collect our spectrum results in section IV that contains subsections on quark mass tuning (IV A), Hartree-Fock calculation of two light quark in the presence of a heavy quark (IV B), tetraquark spectra (IV C) and GEVP analysis (IV D). Finally we summarized our results in section V.

II. QUARK ACTIONS

Lattice QCD simulations with quarks require quark mass to be $am_l \ll 1$, where a is the lattice spacing. In the units of the lattice spacings presently available, the b quark mass is not small *i.e.* $am_b \not\prec 1$. As is generally believed, the typical velocity of a b quark inside a hadron is nonrelativistic $v^2 \sim 0.1$ and is much smaller than the bottom mass. This makes NRQCD our action of choice for b quarks on lattice. We have used $\mathcal{O}(v^6)$ NRQCD action [23], where the Hamiltonian is $H = H_0 + \delta H$, where H_0 is the leading $\mathcal{O}(v^2)$ term, the $\mathcal{O}(v^4)$ and $\mathcal{O}(v^6)$ terms are in δH with coefficients c_1 through c_7 ,

$$H_0 = -\frac{\tilde{\Delta}^2}{2m_b} - \frac{a}{4n} \frac{(\Delta^2)^2}{4m_b^2} \quad (1)$$

$$\begin{aligned} \delta H = & -c_1 \frac{(\Delta^2)^2}{8m_b^3} + c_2 \frac{ig}{8m_b^2} \left(\tilde{\Delta}^\pm \cdot \vec{E} - \vec{E} \cdot \tilde{\Delta}^\pm \right) - c_3 \frac{g}{8m_b^2} \vec{\sigma} \cdot \left(\tilde{\Delta}^\pm \times \tilde{\vec{E}} - \tilde{\vec{E}} \times \tilde{\Delta}^\pm \right) \\ & - c_4 \frac{g}{2m_b} \vec{\sigma} \cdot \tilde{\vec{B}} - c_5 \frac{g}{8m_b^3} \left\{ \Delta^2, \vec{\sigma} \cdot \vec{B} \right\} - c_6 \frac{3g}{64m_b^4} \left\{ \Delta^2, \vec{\sigma} \cdot \left(\tilde{\Delta}^\pm \times \vec{E} - \vec{E} \times \tilde{\Delta}^\pm \right) \right\} \\ & - c_7 \frac{ig^2}{8m_b^3} \vec{\sigma} \cdot \vec{E} \times \vec{E} \end{aligned} \quad (2)$$

where Δ^\pm and Δ^2 are discretized symmetric covariant derivative and lattice Laplacian respectively. Both the derivatives are $\mathcal{O}(a^4)$ improved as are the chromoelectric \vec{E} and chromomagnetic \vec{B} fields. The b quark propagator is generated by time evolution of the Hamiltonian H ,

$$G(\vec{x}, t+1; 0, 0) = \left(1 - \frac{aH_0}{2n}\right)^n \left(1 - \frac{a\delta H}{2}\right) U_4(\vec{x}, t)^\dagger \left(1 - \frac{a\delta H}{2}\right) \left(1 - \frac{aH_0}{2n}\right)^n G(\vec{x}, t; 0, 0) \quad (3)$$

$$\text{with } G(\vec{x}, t; 0, 0) = \begin{cases} 0 & \text{for } t < 0 \\ \delta_{\vec{x}, 0} & \text{for } t = 0 \end{cases}$$

The tree level value of all the coefficients $c_1, c_2, c_3, c_4, c_5, c_6$ and c_7 is 1. Here n is the factor introduced to ensure numerical stability at small am_b , where $n > 3/2m_b$ [22].

In NRQCD, the rest mass term does not appear either in the equation (1) or in (2), and therefore, hadron masses cannot be determined from their energies at zero momentum directly from the exponential fall-off of their correlation functions. Instead, we calculate the kinetic mass M_k of heavy-heavy mesons from its energy-momentum relation, which to $\mathcal{O}(p^2)$ is [25],

$$E(p) = E(0) + \sqrt{p^2 + M_k^2} - M_k \quad \Rightarrow \quad E(p)^2 = E(0)^2 + \frac{E(0)}{M_k} p^2. \quad (4)$$

where M_k is the kinetic mass of the meson which is calculated considering $E(p)$ at different values of lattice momenta $\vec{p} = 2\vec{n}\pi/L$. The b quark mass is tuned from the spin average of kinetic masses of Υ and η_b , and matching them with the experimental spin average value,

$$M_{b\bar{b}} = \frac{3M_\Upsilon + M_{\eta_b}}{4} \quad (5)$$

The experimental value to which $M_{b\bar{b}}$ is tuned to, however, is not 9443 MeV that is obtained from spin averaging Υ (9460 MeV) and η_b (9391 MeV) experimental masses, but to an appropriately adjusted value of 9450 MeV [26], which we denote as $M_{\text{phys}}^{\text{mod}}$ in the equation (6) below. The hadron mass is then obtained from

$$M_{\text{latt}} = E_{\text{latt}} + \frac{n_b}{2} (M_{\text{phys}}^{\text{mod}} - E_{\text{latt}}^{\eta_b}) \quad (6)$$

where E_{latt} is the lattice zero momentum energy in MeV, n_b is the number of b -quarks in the bottom hadron.

The u/d light quarks comfortably satisfy the criteria $am_l \ll 1$ and, therefore, we can use a relativistic lattice action. We use HISQ action for the u/d quarks, which is given in [24],

$$\mathcal{S} = \sum_x \bar{q}(x) (\gamma^\mu D_\mu^{\text{HISQ}} + m) q(x) \text{ where, } D_\mu^{\text{HISQ}} = \Delta_\mu(W) - \frac{a^2}{6}(1 + \epsilon) \Delta_\mu^3(x). \quad (7)$$

Because HISQ action reduces $\mathcal{O}(\alpha_s a^2)$ discretization error found in Asqtad action, it is well suited for u/d (and s) quarks. The parameter ϵ in the coefficient of Naik term can be appropriately tuned to use the action for c quarks, which we do not have here. For u/d (and s) quarks, the $\epsilon = 0$.

HISQ action is diagonal in spin space, and therefore, the corresponding quark propagators do not have any spin structure. The full 4×4 spin structure is regained by multiplying the propagators by Kawamoto-Smit multiplicative phase factor [27],

$$\Omega(x) = \prod_{\mu=1}^4 (\gamma_\mu)^{x_\mu} = \gamma_1^{x_1} \gamma_2^{x_2} \gamma_3^{x_3} \gamma_4^{x_4}. \quad (8)$$

III. TETRAQUARK OPERATORS

In the present paper, we have considered two kinds of tetraquark operators – the local heavy diquark and light antiquark and molecular meson-meson. The b quark, being nonrelativistic, is expressed in terms of two component field ψ_h . We convert it to a four component spinor Q having vanishing two lower components,

$$Q \equiv \begin{pmatrix} \psi_h \\ 0 \end{pmatrix} \quad (9)$$

which help us to combine b field and relativistic four component light quark fields in the usual way. The heavy-light meson operator, that we will make use of in the operator construction, is written as

$$\mathcal{O}_{hl}(x) = \bar{Q}(x) \Gamma l(x) \quad (10)$$

where $l(x)$ stands for the light quark fields, $\bar{Q} = Q^\dagger \gamma_4$ and depending on pseudoscalar and vector mesons $\Gamma = \gamma_5$ and γ_i respectively.

Because of the vanishing lower components, the states with Q can only be projected to the positive parity states. The local double bottom tetraquark operators that we can

construct for $b\bar{b}\bar{l}_1\bar{l}_2$ system are,

$$\mathcal{O}_{M_1} \equiv \mathcal{O}_{B^*B} = [\bar{l}_1(x)\gamma_i Q(x)] [\bar{l}_2(x)\gamma_5 Q(x)], \quad (11)$$

$$\mathcal{O}_{M_2} \equiv \mathcal{O}_{B^*B^*} = \epsilon_{ijk} [\bar{l}_1(x)\gamma_j Q(x)] [\bar{l}_2(x)\gamma_k Q(x)], \quad (12)$$

$$\mathcal{O}_D \equiv \mathcal{O}_{Q^*\tilde{\pi}} = [Q^T(x)C\gamma_i Q(x)] [\bar{l}_1(x)C\gamma_5 \bar{l}_2^T(x)] \quad (13)$$

where $l_1 \neq l_2$ and $l_1, l_2 \in u, d$. The naming convention above is borrowed from reference [15] but the exact construction of the operators is different. In literature the operators in (11) and (12) are often referred to as “molecular”. The quark fields within the square brackets are color contracted. The diquark-antidiquark 1^+ four quark state $b\bar{b}\bar{l}_1\bar{l}_2$ with $l_1 \neq l_2$ in (13) can actually be defined in two ways [28],

$$\begin{aligned} \mathcal{O}_{Q^*\tilde{\pi}} &= [Q^{aT}C\gamma_i Q^b] [\bar{l}_1^a C\gamma_5 \bar{l}_2^{bT} - \bar{l}_1^b C\gamma_5 \bar{l}_2^{aT}] \\ \mathcal{O}_{Q\tilde{\pi}^*} &= [Q^{aT}C\gamma_5 Q^b] [\bar{l}_1^a C\gamma_i \bar{l}_2^{bT} + \bar{l}_1^b C\gamma_i \bar{l}_2^{aT}] \end{aligned} \quad (14)$$

where a, b are color indices. The subscripts Q^* and $\tilde{\pi}$ in the operator $\mathcal{O}_{Q^*\tilde{\pi}}$ are in $\bar{3}_c$ and 3_c respectively, while Q and $\tilde{\pi}^*$ in the operator $\mathcal{O}_{Q\tilde{\pi}^*}$ are in 6_c and $\bar{6}_c$. But both $\mathcal{O}_{Q^*\tilde{\pi}}$ and $\mathcal{O}_{Q\tilde{\pi}^*}$ correspond to the 1^+ state. Of these the $\mathcal{O}_{Q^*\tilde{\pi}}$ is our desired “bound” tetraquark operator because one-gluon-exchange interaction is attractive for a heavy quark pair in $\bar{3}_c$ diquark configuration [8] and spin dependent attraction exists for light quark pairs in “good diquark” configuration characterized by color $\bar{3}_c$, spin $J = 0$ and isospin $I = 0$ or $1/2$ [29]. The two terms in $\mathcal{O}_{Q^*\tilde{\pi}}$ contribute identically in the final correlator, hence we consider only the first term in the calculation. The generic form of the temporal correlation among the operators at zero momentum is,

$$C_{XY}(t) = \sum_{\mathbf{x}} \langle [\mathcal{O}_X(\mathbf{x}, t)] [\mathcal{O}_Y(\mathbf{0}, 0)]^\dagger \rangle, \quad (15)$$

where X, Y can be any of D, M_1, M_2 in equations (11), (12) and (13). For example, the explicit forms of the zero momentum correlators, including cross-correlator, when X and Y

are $M_1 = B^*B$ and $D = \mathcal{Q}^*\tilde{\pi}$, are

$$C_{M_1 M_1}(t) = \sum_{\vec{x}} \text{Tr} \left[\gamma_5 M_1^\dagger(x, 0) \gamma_5 \gamma_i G(x, 0) \gamma_i \right] \times \text{Tr} \left[M_2^\dagger(x, 0) G(x, 0) \right] \quad (16)$$

$$C_{D D}(t) = \sum_{\vec{x}} \text{Tr} \left[(G^{ad}(x, 0))^T \gamma_i \gamma_4 \gamma_2 G^{bc}(x, 0) \gamma_4 \gamma_2 \gamma_i \right] \times \text{Tr} \left[\gamma_4 \gamma_2 M_1^{\dagger da}(x, 0) \gamma_4 \gamma_2 \left(\gamma_5 M_2^{\dagger cb}(x, 0) \gamma_5 \right)^T \right] \quad (17)$$

$$C_{D M_1}(t) = \sum_{\vec{x}} \text{Tr} \left[G^{ad}(x, 0) \gamma_i \gamma_5 M_1^{\dagger da}(x, 0) \gamma_5 \gamma_2 \gamma_4 \gamma_5 \right] \times \text{Tr} \left[\gamma_2 \gamma_i \gamma_4 G^{bc}(x, 0) \gamma_5 \gamma_5 M_2^{\dagger cb}(x, 0) \gamma_5 \right] \quad (18)$$

Above in the equations (17) and (18), traces and transposes are taken over the spin indices, while in the equation (16) the traces are taken over both the spin and color indices. Here $G(x, 0)$ denotes the heavy quark propagators while the $M(x, 0)$ are the light quark propagators. In terms of coding, we have to keep in mind that NRQCD and MILC library suit uses different representation of gamma matrices. Therefore the heavy quark propagator $G(x, 0)$ has to be rotated to the MILC basis before implementing the equations (16), (17) and (18). The unitary matrix needed to do this transformation is given by [30],

$$S \gamma_\mu^{\text{MILC}} S^\dagger = \gamma_\mu^{\text{NR}} \quad \text{where, } S = \frac{1}{\sqrt{2}} \begin{pmatrix} \sigma_y & \sigma_y \\ -\sigma_y & \sigma_y \end{pmatrix}. \quad (19)$$

IV. NUMERICAL STUDIES

We calculated the double bottom tetraquark spectra using the publicly available $N_f = 2 + 1$ Asqtad gauge configurations generated by MILC collaboration. Details about these lattices can be found in [31]. It uses Symanzik-improved Lüscher-Weisz action for the gluons and Asqtad action [32, 33] for the sea quarks. The lattices we choose have a fixed ratio of $am_l/am_s = 1/5$ with lattice spacings 0.15 fm, 0.12 fm and 0.09 fm and they correspond to the same physical volume. We have not determined the lattice spacings independently but use those given in [31]. In the Table I we listed the ensembles used in this work.

A. Quark mass tuning

For $bb\bar{u}\bar{d}$ mass calculation, we need nonperturbative tuning of both m_b and $m_{u/d}$. With the help of equation (5), the tuning of m_b has been carried out by calculating the spin

TABLE I: MILC $N_f = 2 + 1$ Asqtad configurations used in this work. The gauge coupling is β and the lattice spacing is a . The u/d and s sea quark masses are m_l and m_s respectively and the lattice size is $L^3 \times T$. The N_{cfg} is number of configurations used in this work.

$\beta = 10/g^2$	$a(\text{fm})$	am_l	am_s	$L^3 \times T$	N_{cfg}
6.572	0.15	0.0097	0.0484	$16^3 \times 48$	600
6.76	0.12	0.0100	0.0500	$20^3 \times 64$	600
7.09	0.09	0.0062	0.0310	$28^3 \times 96$	300

average Υ and η_b kinetic masses and comparing the same with the spin average and suitably adjusted experimental Υ and η_b masses as discussed in section II. The tuned bare am_b quark masses for lattices used in this work are given in Table II.

TABLE II: Tuned b and u/d quark bare masses for lattices used in this work. For u/d -quark mass, we mention the particle states used to tune.

Quark	Tuning	$16^3 \times 48$	$20^3 \times 64$	$28^3 \times 96$
	hadron	(0.15 fm)	(0.12 fm)	(0.09 fm)
am_b	$\Upsilon - \eta_b$	2.76	2.08	1.20
$am_{u/d}$	Λ_b (5620)	0.105	0.083	0.064
$am_{u/d}$	B (5280)	0.155	0.118	0.087

But the tuning of $am_{u/d}$ is rather tricky and the way to achieve this numerically has been discussed in the study of bottom baryon spectra in [30]. In the present paper, we try to understand the light quark tuning in more details with the help of relativised quark model [34, 35] and Hartree-Fock calculation. The basic idea is that $m_{u/d}$ has to be tuned to two different values corresponding to two different construction of the pairs $[\bar{u}\bar{d}]$ and $[b\bar{u}]$. In the operator $\mathcal{O}_D \equiv [bb][\bar{u}\bar{d}]$, the antidiquark part formed with two light u/d quarks is same as in $\Lambda_b \equiv (u^T C \gamma_5 d) b$, and therefore, we use experimental Λ_b mass 5620 MeV to tune the bare $am_{u/d}$. For the operators \mathcal{O}_{M_1/M_2} , the diquark part is formed between heavy quark and light antiquark $[b\bar{u}]$ which is same as in the B -meson $(\bar{b}\gamma_{(5,k)} u)$ or $\Sigma_b \equiv (Q^T C \gamma_5 u) u$. In such case

we tend to use B -meson mass 5279 MeV to tune the $am_{u/d}$. The result of u/d quark mass tuning that are made use of in this work is given in the Table II.

Before we calculate the spectra of the D , M_1 , M_2 tetraquark states, in the following subsection IV B we try to understand the diquark dependent different tuning of the light u/d quark masses. For this we consider Schrödinger Hamiltonian for (a) hydrogen-like system, namely B meson with an \bar{u} antiquark in the potential of a static b quark and (b) helium-like system, which is Λ_b baryon with \bar{u}, \bar{d} quarks in the same b quark field.

B. Hartree-Fock calculation of tetraquark states

In order to gain a qualitative understanding of two different tunings of $m_{u/d}$, we consider the light antiquark and light-light diquark in the potential of heavy, nearly static color source, the b quark(s). This picture is akin to hydrogen and helium-like quantum mechanical systems. For the molecular tetraquark states, the basic assumption is that the light antiquark wave functions do not have significant overlap with each other and they are effectively in the potential of their respective heavy b quarks [19] i.e. a two B -meson like system. But for the diquark-antidiquark tetraquark state $[bb][\bar{u}\bar{d}]$ where antidiquark component is similar to the Λ_b light-light diquark, we tune the u/d quark mass using the Λ_b baryon. The situation is depicted schematically in Figs. 1 and 2. The relevant interpolating operators for Λ_b and B meson are fairly standard but for HISQ light quarks a whole array of bottom baryon operators, including Λ_b can be found in [30].

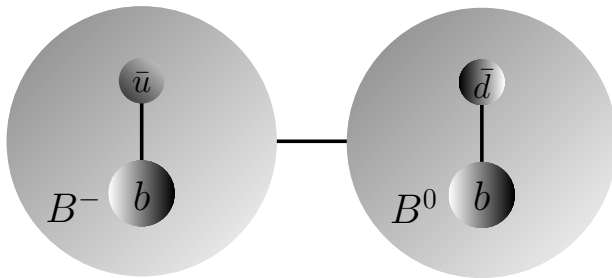


FIG. 1: Molecular tetraquark state viewed as bound state of two B mesons, which is similar to two hydrogen atoms forming a hydrogen molecule.

The relativised quark model [34, 35] helps us to numerically calculate the masses of B meson and Λ_b baryon using the light (anti)quark mass as parameter. The molecular tetraquark state can be visualized as two B meson molecule as shown in the Fig. 1. Then for each B meson, the light u/d antiquark is taken to be in the field of “static” b quark and we solve the problem by considering the radial part of the Schrödinger equation numerically using suitably modified Herman-Skillman code [36].

$$-\frac{1}{2m_{u/d}} \frac{d^2U(r)}{dr^2} + V(r)U(r) = EU(r) \quad (20)$$

Here $U(r) = r\psi(r)$ and the potential $V(r)$ is given by

$$V(r) = -\frac{4\alpha}{3r} + \beta r \quad (21)$$

The B meson mass M_B is, therefore, determined from the energy eigenvalue E ,

$$M_B = m_b + m_{u/d} + E \quad (22)$$

where $m_b = 4.18$ GeV ($\overline{\text{MS}}$) is the mass of the bottom quark, the $\alpha = \pi/16$ [20] and $\beta = 0.18$ GeV² [34]. For $M_B = 5.279$ GeV, the light quark mass obtained is $m_{u/d} \approx 0.227$ GeV.



(a) u/d quarks in Λ_b baryons form a $\bar{3}_c$ diquark in presence of a b quark. (b) Like Λ_b , two b quarks form a (nearly) static nucleus surrounded by \bar{u}, \bar{d} cloud.

FIG. 2: Schematic diagram of helium-like Λ_b and $[bb][\bar{u}\bar{d}]$ tetraquark state used for Hartree-Fock treatment.

For Λ_b baryon, we used Hartree-Fock method [37, 38] to solve the helium-like Hamiltonian,

$$H = -\frac{1}{2m_{u/d}} \nabla_1^2 - \frac{2\alpha}{3r_1} + \frac{\beta r_1}{2} - \frac{1}{2m_{u/d}} \nabla_2^2 - \frac{2\alpha}{3r_2} + \frac{\beta r_2}{2} - \frac{2\alpha'}{3r_{12}} + \frac{\beta' r_{12}}{2} \quad (23)$$

where r_{12} is the relative distance between two light quarks “orbiting” the two heavy quarks and their interaction potential is the last two terms in the equation (23) with coefficient α' and β' . For the Hartree-Fock calculation of the energy E , we take $\beta' = \beta$ and $\alpha' = 0.6$ [34].

To solve the Hamiltonian (23), we consider the trial wave function, which is space-symmetric and spin-antisymmetric, in terms of Slater determinant

$$\Psi^{\text{HF}} = \frac{1}{\sqrt{2}} \begin{vmatrix} \chi_1(x_1) & \chi_1(x_2) \\ \chi_2(x_1) & \chi_2(x_2) \end{vmatrix}, \quad (24)$$

where $x_i \equiv (\vec{r}, s)$ collectively denotes the space and spin indices, $\chi_i(\vec{r}, s) = \phi_{is}(\vec{r}) \mathcal{S}(s)$ with $\phi(\vec{r})$ being the 1S state. Therefore, the expectation value of the the Hamiltonian can be written as

$$\begin{aligned} \langle \Psi^{\text{HF}} | H | \Psi^{\text{HF}} \rangle &= \langle T \rangle + \int \rho(\vec{r}) V_{\text{ext}}(\vec{r}) d\vec{r} - \frac{Z'}{2} \iint \frac{\rho(\vec{r}) \rho(\vec{r}_1)}{|\vec{r} - \vec{r}_1|} d\vec{r} d\vec{r}_1 \\ &+ \frac{B'}{2} \iint \rho(\vec{r}) \rho(\vec{r}_1) |\vec{r} - \vec{r}_1| d\vec{r} d\vec{r}_1 \\ &+ \frac{Z'}{2} \sum_{i,j,s} \iint \frac{\phi_{is}^*(\vec{r}) \phi_{js}^*(\vec{r}_1) \phi_{is}(\vec{r}_1) \phi_{js}(\vec{r})}{|\vec{r} - \vec{r}_1|} d\vec{r} d\vec{r}_1 \\ &- \frac{B'}{2} \sum_{i,j,s} \iint \phi_{is}^*(\vec{r}) \phi_{js}^*(\vec{r}_1) \phi_{is}(\vec{r}_1) \phi_{js}(\vec{r}) |\vec{r} - \vec{r}_1| d\vec{r} d\vec{r}_1 \end{aligned} \quad (25)$$

where, we have used

$$\begin{aligned} \langle T \rangle &= \sum_{i,s} \left\langle \phi_{is}(\vec{r}) \left| -\frac{1}{2m_{u/d}} \nabla^2 \right| \phi_{is}(\vec{r}) \right\rangle \\ \rho(\vec{r}) &= \sum_{i,s} |\phi_{is}(\vec{r})|^2, \quad V_{\text{ext}}(\vec{r}) = -\frac{2\alpha}{3r} + \frac{\beta r}{2} \\ Z' &= \frac{2\alpha'}{3} \quad \text{and} \quad B' = \frac{\beta'}{2}. \end{aligned}$$

In contrast to the helium atom, the presence of linear r -terms in the Hamiltonian leads to additional exchange-energy terms in the calculation. With these linear r -terms in, the Hartree-Fock equation becomes

$$\begin{aligned} E \phi_{is}(\vec{r}) &= \left[-\frac{1}{2m_{u/d}} \nabla^2 + V_{\text{ext}}(\vec{r}) - Z' \int \frac{\rho(\vec{r}_1)}{|\vec{r} - \vec{r}_1|} d\vec{r}_1 + B' \int \rho(\vec{r}_1) |\vec{r} - \vec{r}_1| d\vec{r}_1 \right] \phi_{is}(\vec{r}) \\ &- B' \sum_{j,s} \int \phi_{js}^*(\vec{r}_1) \phi_{is}(\vec{r}_1) \phi_{js}(\vec{r}) |\vec{r} - \vec{r}_1| d\vec{r}_1 \\ &+ Z' \sum_{j,s} \int \frac{\phi_{js}^*(\vec{r}_1) \phi_{is}(\vec{r}_1) \phi_{js}(\vec{r})}{|\vec{r} - \vec{r}_1|} d\vec{r}_1 \end{aligned} \quad (26)$$

We solve for E in equation (26) iteratively and, eventually, the Λ_b mass is calculated from

$$M_{\Lambda_b} = m_b + 2m_{u/d} + E \quad (27)$$

The PDG value of $\Lambda_b(5620)$ is obtained by setting the $m_{u/d}$ to 0.157 GeV.

TABLE III: Comparison of $m_{u/d}$ obtained from various lattices with quark mass parameters in the equations (20) and (26).

Lattice	B meson: $m_{u/d} = 227$ MeV		Λ_b baryon: $m_{u/d} = 157$ MeV	
	$am_{u/d}$	$m_{u/d}$ (MeV)	$am_{u/d}$	$m_{u/d}$ (MeV)
$16^3 \times 48$	0.155	204	0.105	138
$20^3 \times 64$	0.118	194	0.083	137
$28^3 \times 96$	0.087	191	0.064	143

In Table III, we compare the nonperturbatively tuned $m_{u/d}$ on our lattices with those obtained by solving the equations (20) and (26). The bare lattice light quark masses cannot be directly compared to the parameter $m_{u/d}$ in these equations mainly because of the use of renormalized b quark mass (in $\overline{\text{MS}}$ scheme) in the Hartree-Fock calculation. Therefore, the $m_{u/d}$'s in the above calculation return a sort of “renormalized constituent” quark mass. Nonetheless it is obvious that we need two different $m_{u/d}$ for two different systems, namely B and Λ_b . So by comparing the two sets, we simply wish to point out that the lattice tuned $m_{u/d}$'s are in same order of magnitude as Schrödinger equation based quark model but have a difference of 10 – 15%. This helps us to understand the possible physics behind two different tuning of light quark mass in determining the masses of single bottom hadron(s) and double bottom tetraquark states.

C. $bb\bar{u}\bar{d}$ spectrum

A plot of variation of $bb\bar{u}\bar{d}$ mass with various $am_{u/d}$, including the Λ_b and B tuned values is shown in Fig. 3. Here we make a naive comparison of our data with the earlier quark model, lattice calculations and the PDG values, and it shows an interesting trend.

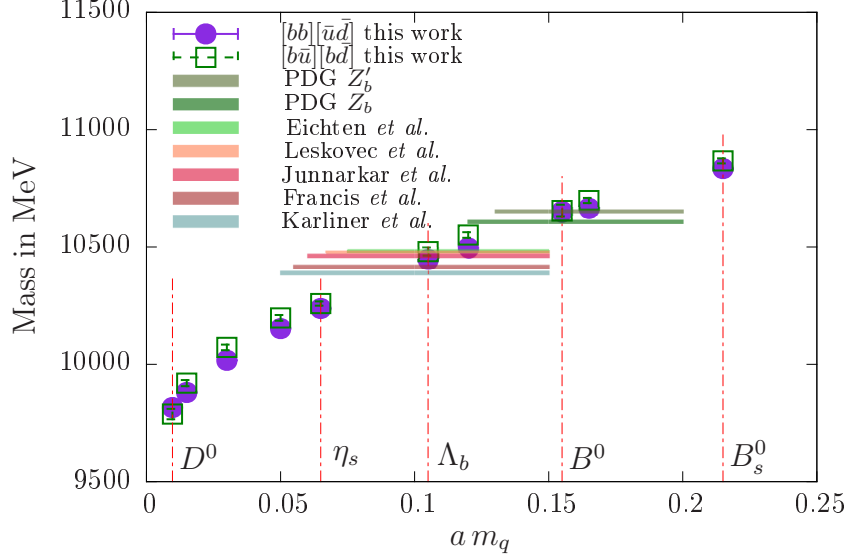


FIG. 3: Variation of $bb\bar{u}\bar{d}$ mass at various $am_{u/d}$ in $16^3 \times 48$ lattice. Λ_b -tuned tetraquark states almost overlap with many of the quark model and lattice calculations, namely Eichten *et al.* [8], Leskovec *et al.* [17], Junnarkar *et al.* [16], Francis *et al.* [14, 15], Karliner *et al.* [39]. The B -tuned states instead coincide with Z_b , Z'_b PDG results [40].

Firstly, PDG Z_b , Z'_b and the lattice results are clustered around two different masses. Our data at B meson tuning point coincides with the PDG Z_b (10610) and Z'_b (10650) states aligning with the idea that they decay mostly into $\bar{B}B^*$ and \bar{B}^*B^* respectively, possibly indicating molecular nature of the state. However, our tetraquark state with Λ_b tuning overlaps mostly with other lattice results indicating the possibility of capturing a bound tetraquark state $[bb][\bar{l}_1\bar{l}_2]$ much like the $b[l\bar{l}]$ state of Λ_b . The effective masses of the states, obtained from \mathcal{O}_D and \mathcal{O}_{M_1} , when compared with the $B - B^*$ threshold, we find D to exhibit a *shallow* bound state while M_1 is just marginally above. The majority of the lattice results [14–17] are found to be below this threshold as is obvious from the Fig. 3.

To this end, in Fig. 4 we plot the effective masses of these two states obtained at different lattice spacings together with the lattice thresholds for easy comparison. The colored bands represent fitted am_{eff} values. The superscripts Λ_b and B denote the light quark tuning.

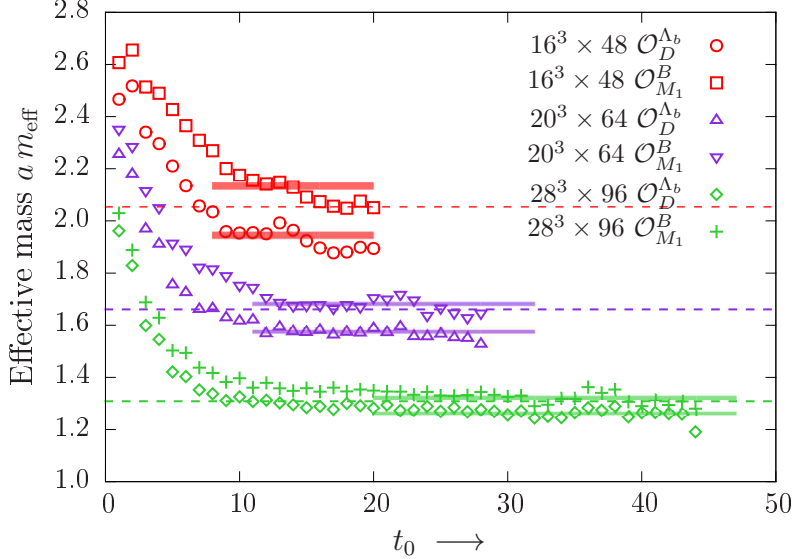


FIG. 4: Effective mass plot of the states of the operators \mathcal{O}_D and \mathcal{O}_{M_1} calculated on $16^3 \times 48$, $20^3 \times 64$ and $28^3 \times 96$ lattices. Dashed lines are $B - B^*$ thresholds for different lattices. For easy viewing, the effective masses and thresholds on $20^3 \times 64$ (purple colored) are multiplied by a common factor of 0.85, while that of $28^3 \times 96$ (green colored) by 0.70.

In the Table IV, we present our results of the tetraquark states corresponding to the operators given in the expressions (11, 12, 13). We use two-exponential uncorrelated fit to the correlation functions, the fitting range being chosen by looking at the positions of what we consider plateau in the effective mass plots. In the columns showing various lattices, we present the masses both in lattice unit $a E_{\text{latt}}$ and physical unit M_{latt} in MeV, the notations being introduced in equation (6). The errors quoted are statistical, calculated assuming the lattice configurations of different lattice spacings are statistically uncorrelated. The second column shows the tuning used for the corresponding states. In the last column we provide the masses averaged over all the lattice ensembles.

From the Fig. 4 and Table IV it is clear that the trial state generated by our \mathcal{O}_D operator is below $B - B^*$ threshold which possibly indicates a bound state. On the other hand, the states for \mathcal{O}_{M_1} and \mathcal{O}_{M_2} are just above it. We tabulate the difference of the masses from the their respective thresholds $\Delta M_{D/M_1/M_2} = M_{D/M_1/M_2} - M_B - M_{B^*}$ in the Table V. In this table, we calculated the following correlator ratio to determine the mass differences which

TABLE IV: Masses of tetraquark states for different $am_{u/d}$ tuning in lattice unit aE_{latt} and M_{latt} in MeV. We also include the B and B^* states that are used for threshold calculation.

Operators	Tuning	$16^3 \times 48$		$20^3 \times 64$		$28^3 \times 96$		Average (MeV)
		aE_{latt}	M_{latt}	aE_{latt}	M_{latt}	aE_{latt}	M_{latt}	
$\mathcal{O}_D = [bb][\bar{u}\bar{d}]$	Λ_b	1.944(5)	10418(7)	1.852(3)	10422(5)	1.803(5)	10407(11)	10417(9)
$\mathcal{O}_{M_1} = [b\bar{u}][b\bar{d}]$	B	2.133(7)	10667(10)	1.977(4)	10628(5)	1.892(6)	10602(13)	10638(27)
$\mathcal{O}_{M_2} = \epsilon_{ijk} [b\bar{u}]_j [b\bar{d}]_k$	B	2.124(7)	10655(8)	1.974(4)	10623(5)	1.890(5)	10560(10)	10623(35)
$B = b\gamma_5\bar{u}$	B	1.022(3)	5274(4)	0.974(3)	5290(3)	0.931(3)	5268(3)	5279(10)
$B^* = b\gamma_k\bar{u}$	B^*	1.032(3)	5288(4)	0.980(3)	5300(4)	0.938(2)	5284(3)	5292(8)

gives us an estimate of the binding energy,

$$C_{X-B-B^*}(t) = \frac{C_X(t)}{C_B(t) \times C_{B^*}(t)} \sim e^{-(M_X - M_B - M_{B^*})t} \quad (28)$$

TABLE V: Mass differences of “bound” D and “molecular” M_1 , M_2 states from $B - B^*$ threshold. The X subscript denotes any of the D , M_1 , M_2 .

Operators	Lattices	$a \Delta M_X$	ΔM_X in MeV	$\overline{\Delta M_X}$ (MeV)
\mathcal{O}_D	$16^3 \times 48$	-0.125(12)	-164(16)	-167(19) this work
	$20^3 \times 64$	-0.108(10)	-177(16)	-215(12) [39]
	$28^3 \times 96$	-0.070(10)	-155(22)	-189(10) [14]
				-143(34) [16]
				-128(34) [17]
\mathcal{O}_{M_1}	$16^3 \times 48$	0.070(12)	92(16)	65(29) this work
	$20^3 \times 64$	0.026(11)	43(18)	see Table VI [17]
	$28^3 \times 96$	0.024(9)	53(20)	
\mathcal{O}_{M_2}	$16^3 \times 48$	0.070(16)	92(21)	63(30) this work
	$20^3 \times 64$	0.022(9)	36(20)	
	$28^3 \times 96$	0.020(10)	44(21)	

In the last column, we calculate our lattice average of ΔM_X in MeV and compare with some of the previous lattice results. To our knowledge, the binding energies of the M_1 , M_2 states have been calculated in the framework of chiral quark model [41] for $B - \bar{B}^*$ and $B^* - \bar{B}^*$ states but there are no lattice results. But the binding energies for the first excited states, along with the ground states, obtained on different lattice ensembles are given in [17]. Though their tuning of light quark mass is very different compared to ours, still we can use their result as a reference.

Our binding energy for the bound tetraquark state $D = [bb][\bar{u}\bar{d}]$ lies somewhere in the middle of the previously quoted lattice results. Our statistical errors of the molecular states M_1 and M_2 are rather large but still they tentatively indicate non-bound molecular nature of the states. We will revisit the binding energy calculation for the molecular state(s) after variational analysis of the $\mathcal{O}_{M_1} \times \mathcal{O}_{M_2}$ correlation matrix.

As we know, on lattice the operators for states having the same quantum numbers can mix and, therefore, a GEVP analysis can help resolve the issue of mutual overlap of various states on the energy eigenstates. In this work, rather than the energies of the eigenstates, we are more interested to learn the overlap of our trial states, namely D , M_1 and M_2 on the first few energy eigenstates, where $|0\rangle$ is the ground state and $|1\rangle$, $|2\rangle$ etc. are the excited states.

D. Variational analysis

For the 2-bottom tetraquark system with quantum number 1^+ , we consider the three local operators – “good” diquark \mathcal{O}_D , molecular \mathcal{O}_{M_1} and vector meson kind \mathcal{O}_{M_2} as defined above in the expressions (11 – 13) – to capture the ground state ($|0\rangle$, \mathcal{E}_0) and possibly the first excited state ($|1\rangle$, \mathcal{E}_1). Apart from the construction itself, as we have discussed before, one basic difference in these operators is the use of different $m_{u/d}$ for simulation of the tetraquark states – Λ_b tuning for \mathcal{O}_D whereas B tuning for \mathcal{O}_{M_1/M_2} operators.

As is generally understood, these operators are expected to have overlap with the desired ground and excited states of the tetraquark system of our interest. The variational analysis can be performed to determine the eigenvalues and the eigenvectors from the mixed states formed by lattice operators. This is typically achieved by constructing a correlation matrix

involving the lattice operators \mathcal{O}_X ,

$$\begin{aligned} C_{XY}(t) &= \left\langle \mathcal{O}_X(t) \mathcal{O}_Y^\dagger(0) \right\rangle \\ &= \sum_{n=0}^{\infty} \langle \Omega | \mathcal{O}_X(t) | n \rangle \langle n | \mathcal{O}_Y^\dagger(0) | \Omega \rangle e^{-E_n t} \end{aligned} \quad (29)$$

where X, Y can either be all or any two combinations of D, M_1, M_2 in the expressions (11 – 13). The terms $\langle n | \mathcal{O}_X^\dagger | \Omega \rangle$ are the coefficients of expansion of the trial states $\mathcal{O}_X^\dagger | \Omega \rangle$, where $|\Omega\rangle$ is the vacuum state, and written in terms of the energy eigenstates $|n\rangle$ as,

$$\mathcal{O}_X^\dagger | \Omega \rangle = \sum_n |n\rangle \langle n | \mathcal{O}_X^\dagger | \Omega \rangle \equiv \sum_n Z_X^n |n\rangle \quad (30)$$

Presently, we are interested in expressing the energy eigenstates in terms of the trial states to understand the contribution of each to the former. If we confine ourselves to the first few energy eigenstates, we can write

$$|m\rangle = \sum_X v_m^X \mathcal{O}_X^\dagger | \Omega \rangle \Rightarrow \langle l | m \rangle = \delta_{lm} \approx \sum_X v_m^X Z_X^l \quad (31)$$

The v_m^X are equivalent to the eigenvector components obtained by solving a GEVP w.r.t a suitably chosen reference time t_0 [12],

$$C(t) v_m(t, t_0) = \lambda_m(t) C(t_0) v_m(t, t_0). \quad (32)$$

The eigenvalues $\lambda_m(t)$ are directly related to the energy of the m -th state, ground and the first few excited states, of our system through the relation

$$\lambda_m(t) = A_m e^{-\mathcal{E}_m(t-t_0)} \quad (33)$$

The component of eigenvectors $v_m(t, t_0)$ gives information about the relative overlap of the three local operators to the m -th eigenstate. The eigenvectors v_m 's are normalized to 1.

To determine the parameter t_0 , we solve the GEVP and found that the ground and excited state energies are almost independent for $t_0 = 3, 5, 7, 9$ as demonstrated in the Fig. 5. In this plot, we showed our results for B -tuned $am_{u/d}$ for all the operators \mathcal{O}_X but the results are similar with Λ_b tuning and, hence, not shown. We chose $t_0 = 5$ for our calculations.

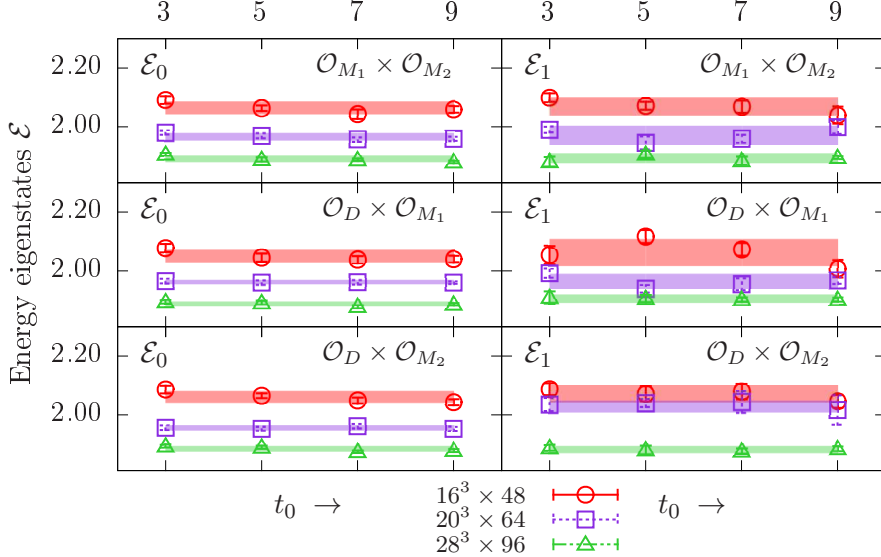


FIG. 5: Variation of ground and excited state energies \mathcal{E}_m of the equation (33) with t_0 , obtained by solving 2×2 GEVP of the correlation matrices $\mathcal{O}_{M_1} \times \mathcal{O}_{M_2}$, $\mathcal{O}_D \times \mathcal{O}_{M_1}$ and $\mathcal{O}_D \times \mathcal{O}_{M_2}$. In this plot we used B -tuned $am_{u/d}$ for all the operators.

TABLE VI: Comparing masses of Λ_b -tuned D (from Table IV) with lowest two energy eigenstates in B -tuned $\mathcal{O}_{M_1} \times \mathcal{O}_{M_2}$ GEVP analysis.

Operators	Energy E-states	16 ³ × 48		20 ³ × 64		28 ³ × 96		ΔM (MeV)
		$a M$	$a \Delta M$	$a M$	$a \Delta M$	$a M$	$a \Delta M$	
\mathcal{O}_D	E_0	1.944(5)	-0.125(12)	1.852(3)	-0.108(10)	1.803(5)	-0.070(10)	-167(19)
$\mathcal{O}_{M_1} \times \mathcal{O}_{M_2}$	\mathcal{E}_0	2.063(10)	0.010(7)	1.959(12)	0.010(9)	1.888(7)	0.012(10)	17(14)
	\mathcal{E}_1	2.071(10)	0.016(6)	1.969(20)	—	1.906(18)	—	

The GEVP analysis has been carried out in two steps because of differences in the tuning of $am_{u/d}$ for the “molecular” states M_1, M_2 and “good” diquark state D . In the Table VI we have shown our GEVP results of $\mathcal{O}_{M_1} \times \mathcal{O}_{M_2}$ correlation matrix and compare the differences of energy level(s) from the threshold with that of D taken from Table IV. However, due to large errors in calculating ΔM in the first excitation \mathcal{E}_1 , we can only reliably quote the lowest energy \mathcal{E}_0 . Here the \mathcal{E}_0 and \mathcal{E}_1 are w.r.t. the $\mathcal{O}_{M_1} \times \mathcal{O}_{M_2}$ correlation matrix. The

ground state energy \mathcal{E}_0 is significantly closer to the threshold than either of M_1 or M_2 . Next we look at the contribution of M_1 and M_2 in constructing the lowest energy eigenstate $|0\rangle$.

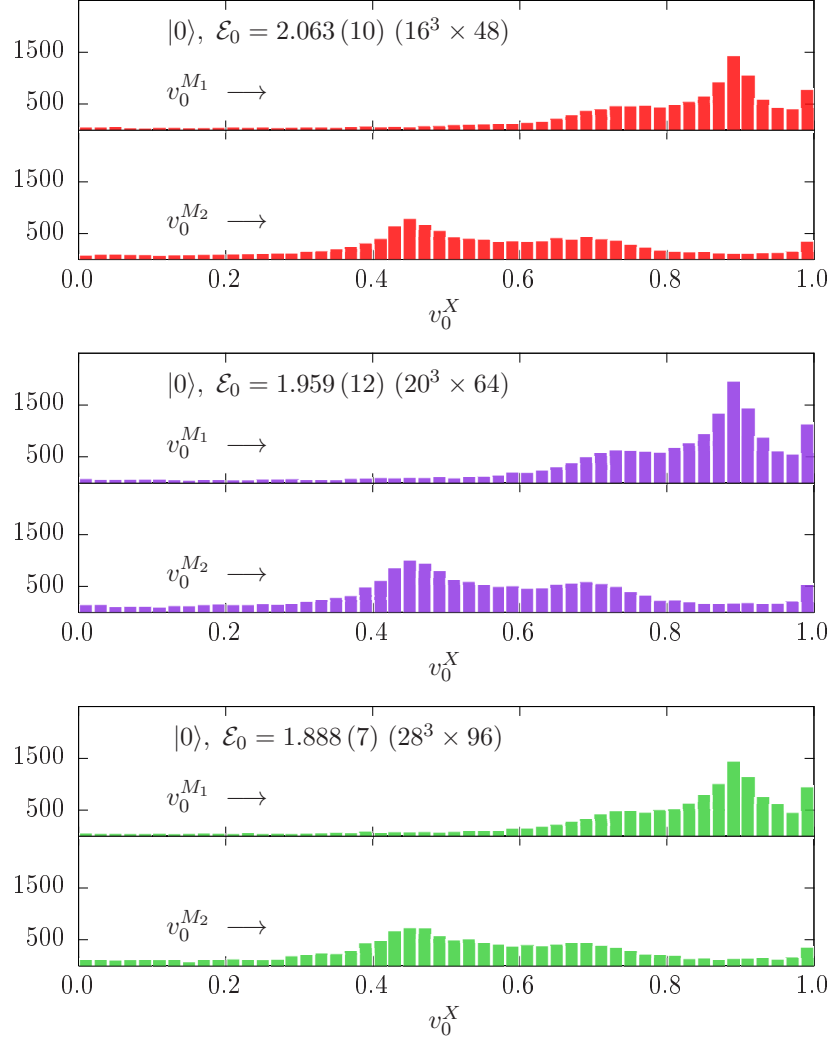


FIG. 6: The histogram plots of the normalized components $(v_0^{M_1}, v_0^{M_2})$ which define the energy eigenstate $|0\rangle = v_0^{M_1}|M_1\rangle + v_0^{M_2}|M_2\rangle$.

In the Fig. 6, we plot the histogram of the components of the normalized eigenvectors $v_0 = (v_0^{M_1}, v_0^{M_2})$ corresponding to the lowest energy \mathcal{E}_0 for all three lattices. Assuming that the coefficients $v_0^{M_1, M_2}$ approximately remain the same on all time slices and for all the individual gauge configurations of an ensemble, the histogram figures are obtained by plotting the M_1, M_2 components of normalized eigenvector v_0 for all time points and individual gauge

configurations. As is expected, all three lattices return identical histogram of the coefficients and hence, in the subsequent histogram plots we will show only the results from $28^3 \times 96$. The eigenvector component $v_0^{M_1}$ shows a peak around 0.9 indicating the lowest energy state $|0\rangle$ receives dominant contribution from M_1 trial state. We recall here that \mathcal{O}_{M_1} corresponds to the $B - B^*$ molecular state as defined in the equation (11).

However, the first excitation $|1\rangle$, for which our data is rather noisy to reliably estimate ΔM , the $|M_1\rangle$ and $|M_2\rangle$ states appear to have comparable contribution and are broadly distributed over different time slices and vary significantly over configurations. This is evident from the histogram plot in the Fig. 7. This may have a bearing with the fact that above the threshold, the Z_b tetraquark can couple to multiple decay channels resulting in a broad spectrum.

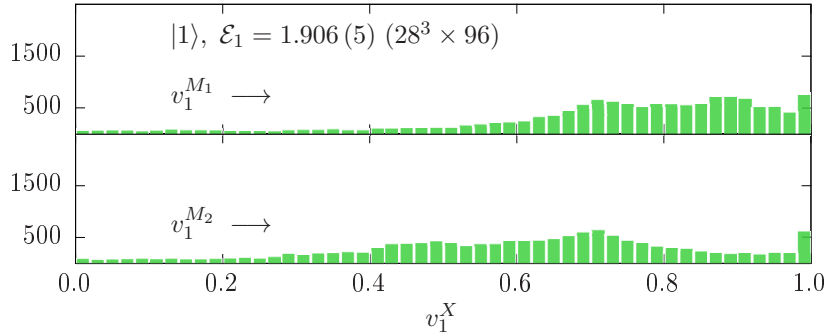


FIG. 7: The histogram plot of $v_1^{M_1}$ and $v_1^{M_2}$ that define the energy eigenstate $|1\rangle = v_1^{M_1}|M_1\rangle + v_1^{M_2}|M_2\rangle$.

Including \mathcal{O}_D along with the \mathcal{O}_{M_1} and \mathcal{O}_{M_2} to form a 3×3 correlation matrix requires using either Λ_b or B tuned $am_{u/d}$ in all three trial states. An important issue here is to interpret what Λ_b tuning meant for $B - B^*$ meson system or, conversely, what B tuning is meant for Λ_b like system. Certainly, a B -tuned bound D state above threshold is not well-defined and we find it has statistically small and varying overlap with the energy eigenstates much like in Fig. 7. On the other hand, Λ_b tuned molecular states can possibly have finite overlap to the eigenstates below threshold. However, we always expect dominance of D in $|0\rangle$ because of the difference in construction of wave functions of the M_1 and M_2 .

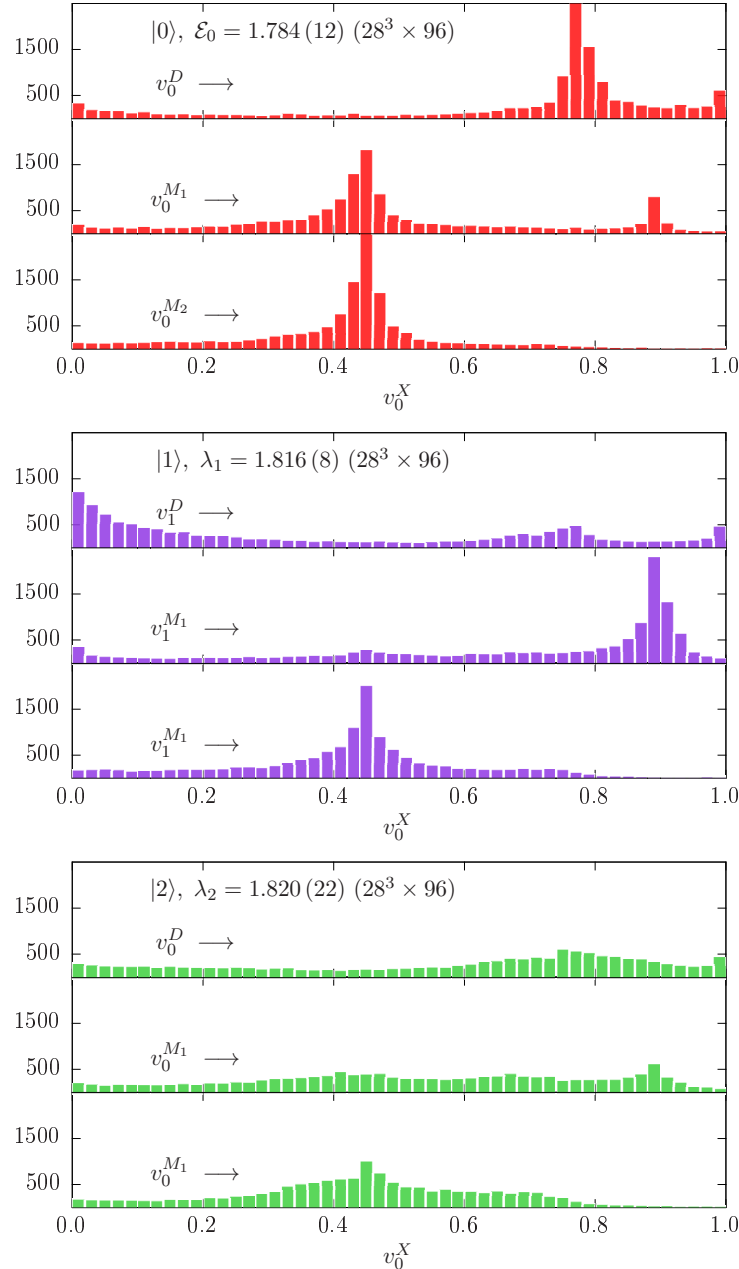


FIG. 8: Histogram plots of the normalized eigenvector components v_0^X , v_1^X and v_2^X of 3×3 correlation matrix, where $X = D, M_1, M_2$, on $28^3 \times 96$ lattice.

The histogram of the eigenvector components of 3×3 correlation matrix are shown in the Fig. 8 for the $28^3 \times 96$ lattices. The lowest energy eigenstate $|0\rangle$ is clearly dominated by D showing peak around 0.8, although it receives sizeable overlap from both M_1 and M_2 peaking around 0.45. But overlap of D on $|1\rangle$ is rather small and it is mostly molecular M_1

despite the excited state energy \mathcal{E}_1 is below the threshold. Our data for $|2\rangle$ is too noisy to extract much information. Based on this Λ_b tuned 3×3 GEVP analysis, the binding energy for the ground state obtained is $-186(15)$ MeV.

V. SUMMARY

In this work we have attempted to study two possible $bb\bar{u}\bar{d}$ tetraquark states – one which is bound and where most other lattice results are centered and, the other which is reported in PDG as Z_b and Z'_b . The experimentally observed states are believed to contain a $b\bar{b}$ pair but ours is bb pair which is considered as theoretically simpler. However, the possible molecular nature of Z_b and Z'_b suggests that our molecular states should have similar masses. For the bottom quarks we have used NRQCD action while HISQ action for the u/d quarks. This NRQCD-HISQ combination has been employed earlier in [26] for bottom meson and recently in [30] for bottom baryons. We have constructed the three lattice 1^+ trial states: a bound D containing “good diquark” 3_c configuration and two meson-meson molecular M_1, M_2 with the expectation that they will contribute to the states above $B - B^*$ threshold. There are not many lattice results on the states above threshold possibly because of the complication that they can couple to multiple decay channels besides $B^*\bar{B}$ and $B^*\bar{B}^*$. Our motivation here is to obtain a tentative estimate of the M_1, M_2 states above threshold and their relative overlap with the bound state below the threshold.

An important component of the present investigation is the tuning of the light u/d quark mass. Depending on the wave function of the operators we need two different tuning of the u/d mass. For the operators made of heavy-light $[b\bar{l}]$ mesonic wave functions we find it is necessary to tune am_l to match $b\bar{l}$ meson observed mass. Similarly, for light-light diquark $[l_1l_2]$, where l_1 and l_2 may or may not be equal, in presence of one or more heavy b quarks the am_{l_i} is tuned with Λ_b . We applied this approach with fair success in bottom baryon [30] and presently with double bottom tetraquark we attempted the same. In order to understand and explain these two different tuning, we solve the quantum mechanical Hamiltonians of B -meson system, where a single light quark is in the potential of a static bottom quark, and the Λ_b -baryon system, where the two light quarks are in the same field of the static b quark. In this problem b mass is the experimental mass and the light quark mass is treated as a parameter which is tuned to reproduce the experimental B and Λ_b masses. We find that

the meson and baryon systems are solved for two different light quark masses which justifies our need for two different tunings. However, the actual numbers from these two sets of light quark masses, one from solving the Schrödinger equation and the other lattice tuned, cannot be compared directly due to two different b masses used in these two instances.

Once tuned, we find the spectra of the lattice states D , M_1 and M_2 . Naive calculation of $\langle \mathcal{O}_D \mathcal{O}_D^\dagger \rangle$ spectrum yields a bound state $-167(19)$ MeV measured from the $B - B^*$ threshold. On lattice, operators for states having the same quantum numbers can mix and, therefore, it is natural to construct correlation matrices to solve the generalized eigenvalue problem in order to obtain the first few lowest lying energies. Besides, the components of the eigenvectors provide the relative contribution of the trial states, corresponding to the lattice operators, to the energy eigenstates. They are the coefficient of expansion of the eigenstates when expressed in terms of trial states as shown in the equation (31). The GEVP analysis reveals that tetraquark molecular state just above the threshold by only $17(14)$ MeV is dominated by M_1 lattice state while the lowest lying bound state receives dominant contribution from D along with significantly large contribution from both M_1 and M_2 . From $3 \times 3 \Lambda_b$ tuned correlation matrix, we get our final binding energy number for $bb\bar{u}\bar{d}$ tetraquark system to be $-186(15)$ MeV, where the error is statistical.

VI. ACKNOWLEDGEMENT

The numerical part of this work, involving generation of heavy quark propagators, has been performed at HPC facility in “Kalinga” cluster at NISER funded by Dept. of Atomic Energy (DAE), Govt. of India. The construction of the correlators and other analysis part of this paper has been carried out in the “Proton” cluster funded by DST-SERB project number SR/S2/HEP-0025/2010. The authors acknowledge useful discussions with Rabeet Singh (Banaras Hindu University, India) on Hartree-Fock calculation. One of the authors (PM) thanks DAE for financial support.

REFERENCES

- [1] A.E. Bondar, A. Garmash, A.I. Milstein, R. Mizuk and M.B. Voloshin, Phys. Rev. D **84**, 054010 (2011).
- [2] A. Bondar *et al.* (Belle Collaboration), Phys. Rev. Lett. **108**, 122001 (2012).
- [3] R. Aaij *et al.* (LHCb Collaboration), Phys. Rev. Lett **112**, 222002 (2014).
- [4] R.F. Lebed, R.E. Mitchell and E.S. Swanson, Prog. Part. Nucl. Phys. **93**, 143 (2017).
- [5] A. Esposito, A. Pilloni and A.D. Polosa, Phys. Rep. **668**, 1 (2017).
- [6] S.L. Olsen, T. Skwarnicki and D. Zieminska, Rev. Mod. Phys. **90**, 015003 (2018).
- [7] A.V. Manohar and M.B. Wise, Nucl. Phys. **B399**, 17 (1993).
- [8] E.J. Eichten and C. Quigg, Phys. Rev. Lett. **119**, 202002 (2017).
- [9] Y. Ikeda, B. Charron, S. Aoki, T. Doi, T. Hatsuda, T. Inoue, N. Ishii, K. Murano, H. Nemura and K. Sasaki, Phys. Lett. **B729**, 85 (2014).
- [10] Marc Wagner *et al.* 2014 J. Phys.: Conf. Ser. **503**, 012031.
- [11] M. Padmanath, C.B. Lang and S. Prelovsek, Phys. Rev. D **92**, 034501 (2015).
- [12] C. Alexandrou, J. Berlin, J. Finkenrath, T. Leontiou and M. Wagner, Phys. Rev. D **101**, 034502 (2020).
- [13] C. Hughes, E. Eichten and C.T.H. Davies, Phys. Rev. D **97**, 054505 (2018).
- [14] A. Francis, R.J. Hudspith, R. Lewis and K. Maltman, Phys. Rev. Lett. **118**, 142001 (2017)
- [15] A. Francis, R.J. Hudspith, R. Lewis and K. Maltman, Phys. Rev. D **99**, 054505 (2019).
- [16] P. Junnarkar, N. Mathur and M. Padmanath, Phys. Rev. D **99**, 034507 (2019).
- [17] L. Leskovec, S. Meinel, M. Pflaumer and M. Wagner, Phys. Rev. D **100**, 014503 (2019).
- [18] P. Bicudo, and M. Wagner, Phys. Rev. D **87**, 114511 (2013).
- [19] P. Bicudo, K. Cichy, A. Peters, B. Wagenbach and M. Wagner, Phys. Rev. D **92**, 014507 (2015).
- [20] P. Bicudo, J. Scheunert and M. Wagner, Phys. Rev. D **95**, 034502, (2017).
- [21] P. Bicudo, M. Cardoso, A. Peters, M. Pflaumer and M. Wagner, Phys. Rev. D **96**, 054510 (2017).
- [22] B.A. Thacker and G.P. Lepage, Phys. Rev. D **43**, 196 (1991).

- [23] G.P. Lepage, L. Magnea, C. Nakhleh, U. Magnea and K. Hornbostel, Phys. Rev. D **46**, 4052 (1992).
- [24] E. Follana, Q. Mason, C. Davies, K. Hornbostel, G.P. Lepage, J. Shigemitsu, H. Trottier and K. Wong, Phys. Rev. D **75**, 054502 (2007).
- [25] A.X. El-Khadra, A.S. Kronfeld and P.B. Mackenzie, Phys. Rev. D **55**, 3933 (1997).
- [26] E.B. Gregory *et al.* (HPQCD Collaboration), Phys. Rev. D **83**, 014506 (2011).
- [27] N. Kawamoto and J. Smit, Nucl. Phys. B **192**, 100 (1981).
- [28] J. Jiang, W. Chen and S. Zhu, Phys. Rev. D **96**, 094022 (2017).
- [29] R.L. Jaffe, Phys. Rep. **409**, 1 (2005).
- [30] P. Mohanta and S. Basak, Phys. Rev. D **101**, 094503 (2020).
- [31] A. Bazavov *et al.*, Rev. Mod. Phys. **82**, 1349 (2010).
- [32] K. Orginos and D. Toussaint (MILC), Phys. Rev. D **59**, 014501 (1998).
- [33] K. Orginos, D. Toussaint, and R. L. Sugar (MILC), Phys. Rev. D **60**, 054503 (1999).
- [34] S. Godfrey and N. Isgur, Phys. Rev. D **32**, 189 (1985).
- [35] S. Capstick and N. Isgur, Phys. Rev. D **34**, 2809 (1986).
- [36] folk.uib.no/nfylk/Hartree/lindex.html
- [37] D. R. Hartree and W. Hartree, Proc. R. Soc. Lond. A150: 933, (1935).
- [38] V. Fock, Z. Physik 61, 126148 (1930).
- [39] Marek Karliner and Jonathan L. Rosner, Phys. Rev. Lett. **119**, 202001 (2017)
- [40] M. Tanabashi *et al.* (Particle Data Group), Phys. Rev. D98, 030001 (2018) and 2019 update.
- [41] G. Yang, J. Ping, and J. Segovia, Phys. Rev. D **101**, 014001 (2020)